# Simulation of gain stability of THGEM gas-avalanche particle detectors

Jinst

Published by IOP Publishing for Sissa Medialab

Received: *November 2, 2017*
Accepted: *January 3, 2018*
Published: *January 19, 2018*

# Simulation of gain stability of THGEM gas-avalanche particle detectors

**P.M.M. Correia,**[a,1,2] **M. Pitt,**[b,2] **C.D.R. Azevedo,**[a] **A. Breskin,**[b] **S. Bressler,**[b] **C.A.B. Oliveira,**[a] **A.L.M. Silva,**[a] **R. Veenhof**[c] **and J.F.C.A. Veloso**[a]

[a] *I3N — Physics Department, University of Aveiro, Campus Universitário de Santiago 3810-193, Aveiro, Portugal*
[b] *Dept. of Astrophysics and Particle Physics, Weizmann Institute of Science, P.O. Box 26, Rehovot 76100, Israel*
[c] *CERN PH department, CH-1211 Genève 23, Switzerland*

*E-mail:* pmcorreia@ua.pt

Abstract: Charging-up processes affecting gain stability in Thick Gas Electron Multipliers (THGEM) were studied with a dedicated simulation toolkit. Integrated with Garfield++, it provides an effective platform for systematic phenomenological studies of charging-up processes in MPGD detectors. We describe the simulation tool and the fine-tuning of the step-size required for the algorithm convergence, in relation to physical parameters. Simulation results of gain stability over time in THGEM detectors are presented, exploring the role of electrode-thickness and applied voltage on its evolution. The results show that the total amount of irradiated charge through electrode's hole needed for reaching gain stabilization is in the range of tens to hundreds of pC, depending on the detector geometry and operational voltage. These results are in agreement with experimental observations presented previously.

Keywords: Detector modelling and simulations II (electric fields, charge transport, multiplication and induction, pulse formation, electron emission, etc); Micropattern gaseous detectors (MSGC, GEM, THGEM, RETHGEM, MHSP, MICROPIC, MICROMEGAS, InGrid, etc)

[1] Corresponding author.
[2] Equal contribution.



https://doi.org/10.1088/1748-0221/13/01/P01015

2018 JINST 13 P01015

## Contents


**1 Introduction** **1**

**2 The simulation toolkit** **2**
2.1 Electric field calculations 2
2.2 Simulations steps 2

**3 Application of the method to THGEMs** **5**
3.1 Simulation setup 5
3.2 Physical interpretation 6
3.3 Convergence rules 7

**4 Results** **8**
4.1 Voltage effect on gain stabilization 8
4.2 Electrode-thickness effect on the gain stabilization 8

**5 Conclusions** **10**


## 1 Introduction

The time-evolution of the avalanche gain in Micro-Patterned Gaseous Detectors (MPGDs) has been a topic of major interest in the last years. Gain variations with time have been reported and are common in detectors containing dielectric materials in contact with the gas medium where multiplication occurs; the effects have been noticed particularly in detectors based on hole-type MPGDs with insulating surfaces in contact with active gases, e.g. Gas Electron Multipliers (GEMs) [1–3] and Thick-GEMs (THGEMs) [4–10].

Gain variation over time in GEM and THGEM-based detectors can arise from different processes, e.g. polarization of the insulator's volume under applied voltage, and charging-up of the insulator's surfaces exposed to the free drifting charges (electrons and ions) in the gas volume [4]. It has been also observed that detector's environmental conditions, such as gas impurities and moisture, can affect gain transients [9].

A simulation program has been developed for phenomenological studies of charging-up effects in GEM detectors [11, 12]. The tool is based on the superposition principle according to which the field inside the holes is the sum of the field prior to any charge accumulating on the insulating surface and the field due to the charge accumulated on the insulators. This simulation tool predicted the time dependence of the gain in the GEM detectors with double-conical holes.

The superposition principle is also used to discuss experimental observation of gain variation over time [9, 13]. In this work, the simulation tools were further improved and extended to THGEM-based detectors. We have focused on the development of a new toolkit that allows for calculations



2018 JINST 13 P01015

of charging-up effects of the detector's insulator surfaces in a more efficient way. The polarization of the insulator volume and its influence on gain evolution were not studied in this document. In the current simulations, the detector was assumed to be biased prior to irradiation.

The present toolkit allows for the simulation of charging-up effects, based on the superposition principle of electric fields. This toolkit, which can be included to Garfield++[14], can be extended to virtually all MPGDs in a straightforward way. It has been applied in this work to the study of gain evolution in THGEM detectors, under typical experimental conditions, and can be downloaded from [15].

## 2 The simulation toolkit

### 2.1 Electric field calculations

To simulate charging-up effect in THGEMs, the method for the charging-up calculations described in [12] was chosen.

The total field $\vec{E}_{\text{tot}}$ can be estimated using the superposition principle

$$\vec{E}_{\text{tot}} = \vec{E}_{\text{uncharged}} + \vec{E}_{\text{charges}} \tag{2.1}$$

Here $\vec{E}_{\text{uncharged}}$ is the electric field resulting from the voltage applied to the THGEM electrodes prior to any charging-up, $\vec{E}_{\text{charges}}$ is the field due to the charges accumulating in the insulator surfaces (electrons and ions). This definition was also at the base of the analysis presented in [9]. While $\vec{E}_{\text{uncharged}}$ remains constant, $\vec{E}_{\text{charges}}$ varies due to the continuous accumulation of charges. Hence, the total field at equilibrium can be obtained in an iterative process, where in each iteration $\vec{E}_{\text{charges}}$ is modified according to the cumulative surface charge.

During the first iteration, that corresponds to the simulation of the multiplication process in a THGEM before irradiation, i.e., prior to charge accumulation on the insulator surfaces, a set of primary avalanches is simulated. A fraction of the free charges (drifting electrons and ions) end up accumulating on the insulator, as depicted in figure 1a. These charges will modify the electric field by some amount, resulting in a new field map, $\vec{E}_{\text{tot}}$, that can be obtained from the superposition of $\vec{E}_{\text{uncharged}}$ and $\vec{E}_{\text{charges}}$, as depicted in figure 1b.

### 2.2 Simulations steps

Previous simulation works related to charging-up effects in MPGDs relied on calculations of the electric field in the region of interest and simulation of the avalanche and detector's gain. The amount of charges produced on the avalanche that ended up trapped on the insulator surfaces was evaluated, a new electric-field map resulting from the addition of these charges was calculated, and the process was repeated, as shown in figure 2. Using this iterative method, the simulation results of the charging-up process were in agreement with experimental data obtained with GEM detectors [12].

The finite element method (FEM), as implemented in **ANSYS®**,[1] is used to calculate the electric potential in the gas volume, which then is used to infer the electric field at a given point of all the avalanche electrons' path [16]. Avalanche-size calculations and transport properties of the charges (electrons and ions) are calculated in Garfield++[14] (which interfaces with Magboltz [17, 18]), that simulates collisions of electrons in a given gas mixture and detector geometry.

[1] http://www.ansys.com.



2018 JINST 13 P01015

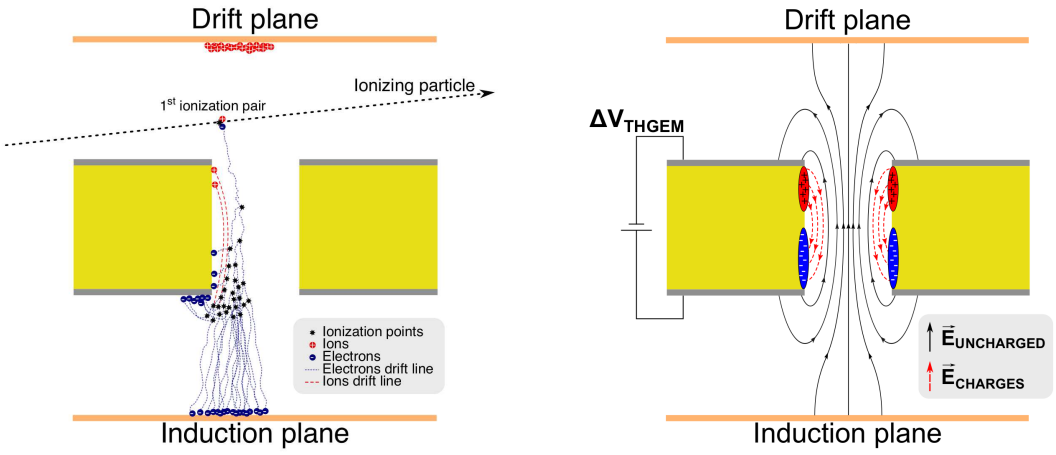


**Figure 1.** (a) Schematic drawing of the charging-up process during an avalanche. (b) Charging-up superposition algorithm of the THGEM: the total electric field is a sum of $\vec{E}_{\text{uncharged}}$, calculated when voltages are applied on the electrodes and the detector was not exposed to ionizing radiation yet, superimposed with the electric field induced by accumulated charges on the insulator's surface of the detector $\vec{E}_{\text{charges}}$.

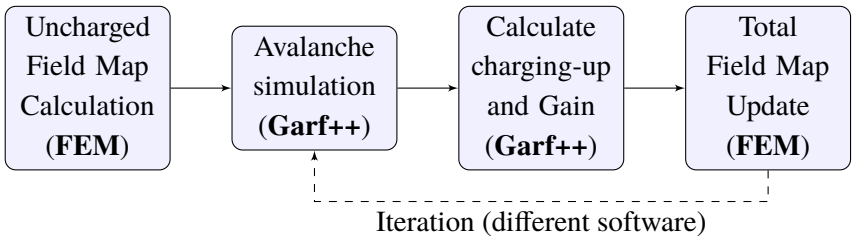


**Figure 2.** Flowchart of the previous simulation method, alternating from FEM back to Garfield++ after each iteration.

The previous implementation of the simulation toolkit was CPU and time consuming. It was based on an iterative transition between the FEM software and Garfield++ after each iteration, as depicted in figure 2. The update of the field-map, according to Garfield++ charge deposition results, required a new FEM calculation — to include the original electric field produced by the voltages applied in the detector as well as that arising from the accumulation of charges on the insulator surfaces. The simulations could take as long as several hundreds days of CPU time for a given gas mixture and amplification voltage. Even the use of parallelism tools (multiple processors, multithread, etc) can only reduce the computing time but not the algorithm efficiency, which sometimes even required manual intervention in the files between iterations.

Hence, in this work we have elaborated a faster solution based in a different algorithm. While in the previous method, the new field-maps between each iterations were calculated in the FEM software, forcing a transition between the FEM software and Garfield++ after each iteration, in the method now described, several field-maps, previously calculated in the FEM software, are imported to Garfield++, and further iterative calculations are performed without running new instances of the FEM software, speeding up the simulations. A schematic description is given in figure 3.



2018 JINST 13 P01015

A new $\vec{E}_{\text{charges}}$ is calculated at the end of each iteration and is used to update $\vec{E}_{\text{tot}}$. The next iteration takes into consideration the updated $\vec{E}_{\text{tot}}$ of the previous iterations. The different electric-field during iterations changes the avalanche process, which influences on the measured gain. Assuming a certain irradiation rate, a time-evolution of the gain can therefore be simulated. A flowchart of the superposition algorithm is depicted in figure 3.

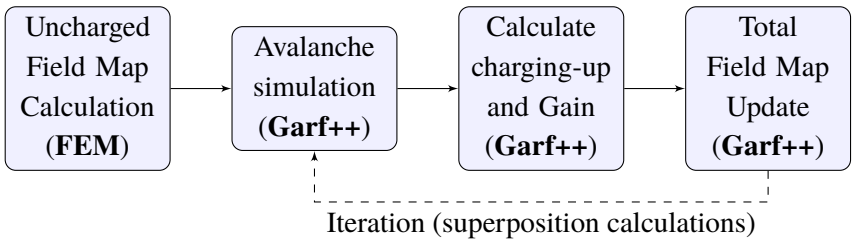


**Figure 3.** Flowchart of the superposition method. Compared with previous flowchart (figure 2), FEM is used only at the beginning of the simulation. All further calculations are performed in Garfield++.

For a THGEM, the following procedure is applied for computing the field maps of interest:

- The THGEM insulator surface is divided into 20 slices as shown in figure 4. The number of slices was choose based on previous studies [12] where a good balance between the slice surface, the electric field distortion due to the slice granularity and to the distribution of the accumulated charges onto the insulating hole's walls (as shown in figure 5b) and the computing power is achieved.
- The $\vec{E}_{\text{uncharged}}$ is calculated from the voltages applied;
- For each slice, a field map, considering only the electric field due to an unitary charge distributed uniformly over the exposed surface of the slice, is calculated — defined here as $\vec{E}_{\text{slices}}$.

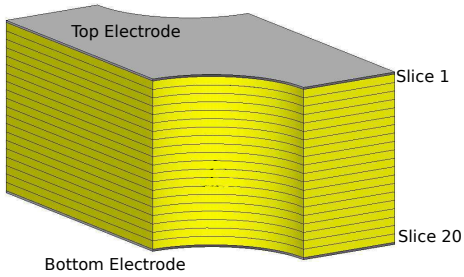


**Figure 4.** The THGEM cell (without a hole-rim) employed in the simulations. The insulator surface is divided into 20 slices along the THGEM hole.

Once these field maps are available, the Garfield++ simulation can start. To perform the simulation, Garfield++ imports the coordinates of the nodes and the associated electric potential as a list. In order to calculate $\vec{E}_{\text{charges}}$, an avalanche is calculated, and the position of all the electrons or ions deposited on an insulating surface is stored. The total number of accumulated charges $N = N_{\text{electrons}} - N_{\text{ions}}$ (the number of accumulated electrons minus that of accumulated ions) is assigned to the corresponding slice. Since the expected variation of the field from $N$ charges on a



2018 JINST 13 P01015

given slice for a single avalanche is very small, for fast algorithm convergence, the total number of accumulated charges attached to a single slice is usually multiplied by a constant value $s$ (*step-size*). Therefore, in the case where $N$ charges have stopped on the surface of a slice $j$ (without other extra charges accumulated in the remaining surfaces), we need to calculate, for each node $i$, the electric potential $V$ for that node which is given by eq. (2.2):

$$V(\text{charges}, i) = V(\text{uncharged}, i) + N \times s \times V(j, i) \tag{2.2}$$

where $V(j, i)$ is the electric potential on node $i$ due to the presence of a unitary positive charge in the surface of slice $j$, calculated from the $\vec{E}_{\text{slices}}$ described previously. Depending on the accumulated charges, $N$ can either be positive (more ions) or negative (more electrons).

Once $\vec{E}_{\text{charges}}$ is calculated, the next iteration is launched. The total electric field is calculated from eq. (2.1). The total electric field updating procedure is repeated until the total amount of accumulated charges $N$ after a given number of iterations is equal to zero — $\vec{E}_{\text{tot}}$ became constant with the increasing number of iterations.

## 3 Application of the method to THGEMs

### 3.1 Simulation setup

With the method described in the previous section, we are able to simulate the charging-up effect using only Garfield++, even though more than one field map has to be introduced as input at the beginning of the simulation.

The THGEM-detector geometry simulated in this work has an electrode with an hexagonal pattern of hole-pitch $a$ = 1 mm, hole diameter $d$ = 0.5 mm, with no rim, and FR4 substrate having a thickness $t$ = 0.4 mm, 0.8 mm and 1.2 mm. Electric fields of 0.2 and 0.5 kV cm$^{-1}$ were set across the drift and induction gaps respectively.

Voltages $\Delta V_{\text{THGEM}}$ were applied across the THGEM electrode. Several gas mixtures were used in the simulations. In most of the cases Ne and Ne/$CH_4$(5%), however to obtain similar electron multiplication at higher voltages, the simulation work was extended to Ar-based gas mixtures: Ar, Ar/$CH_4$ (5%) and Ar/$CO_2$(5,7%). Since some of these are believed to be Penning-mixtures [19], Penning factors of 0.40 for Ne/$CH_4$(5%), 0.18 for Ar/$CH_4$ (5%), 0.35 for Ar/$CO_2$(5%) and 0.4 for Ar/$CO_2$(7%) [20–22] were used. Standard room-temperature conditions were considered ($T$=293 K and $P$=1 bar). A constant irradiation rate of 10 Hz mm$^{-2}$, 8 keV x-rays, was assumed. In our simulations, a random location for primary charges originated by the incoming x-rays is assumed and the charges are drifted towards the THGEM holes from different positions.

At each iteration, the gain for a single-electron avalanche multiplication was calculated. Electron multiplication is a stochastic process, and the gain is determined as the average number of electrons generated during the electron avalanche process. At each iteration a given number of avalanches between 100 and 1000 was simulated (denoted in the text as $n_{\text{AV}}$). In all simulations, the statistical error on the mean gain of the detector was taken to be

$$\frac{\sigma(\text{G})}{\text{G}} = \sqrt{\frac{1}{n_{\text{AV}}}} \tag{3.1}$$



2018 JINST 13 P01015

In each avalanche, the position of all the electrons or ions deposited on an insulating surface is stored, and assigned to the corresponding slice. Electrons that do not end up on the insulator are either collected on the THGEM bottom electrode, on the induction plane, while non-trapped ions end up on the top THGEM electrode or on the drift plane. Some of the electrons are attached to the gas molecules ($CO_2$ or $CH_4$) and are not taken into account in the gain calculation.

### 3.2 Physical interpretation

The number of simulated iterations ($n_{\text{iter}}$) can be translated to a physical irradiation time ($t$) as follows: given the number of primary charges induced in the gas by the ionizing event[2] ($n_{\text{p}}$), the irradiation rate ($R$) and the *step-size* ($s$) can be related to a physical irradiation time:

$$t[\text{sec}] = \frac{s}{n_{\text{p}} \times R\ [\text{Hz}]} \times n_{\text{iter}} \tag{3.2}$$

An example of a simulation result of the gain evolution in a THGEM detector, in Ne/$CH_4$(5%) gas mixture with the parameters: $t$=0.8 mm, $a$=1 mm, $d$=0.5 mm, and no-rim, is shown in figure 5.

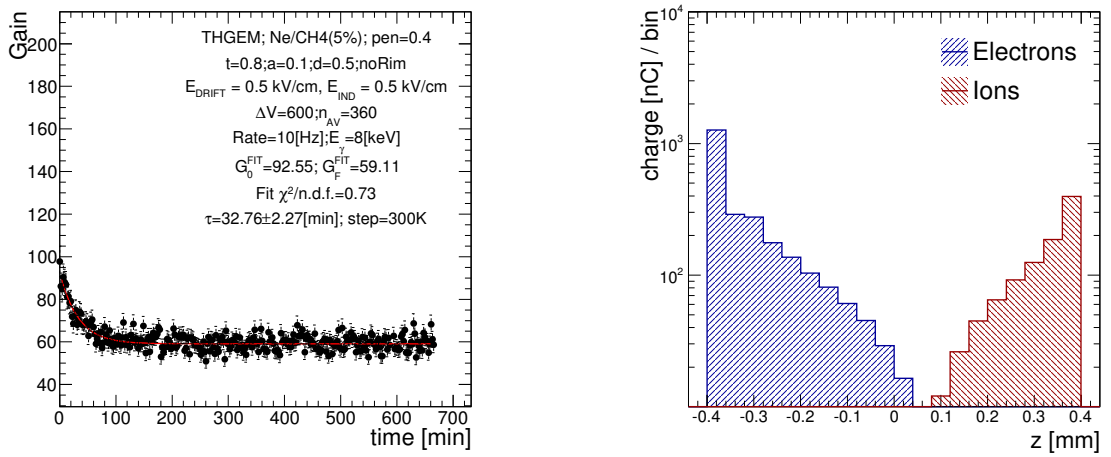


(a) (b)

**Figure 5.** Simulated gain evolution in the THGEM as function of time (a) and the distribution of the accumulated charges onto the insulating hole's walls, along the hole's z-axis (b), in Ne/$CH_4$(5%). The exponential fit in the left figure relies on eq. (3.3). The fitted parameters are shown in the inner caption.

Gain evolution curves over time were fitted using:

$$G(t) = G_0 - \Delta G\left(1 - e^{-t/\tau}\right) \tag{3.3}$$

where $G(t)$ is the gain at a given instant, $G_0$ is the initial gain, $\tau$ is the relaxation time constant (or *characteristic time*), and $\Delta G$ is the gain variation. The final gain, $G_{\text{F}}$, can be calculated in terms of $G_0$ and $\Delta G$:

$$G_{\text{F}} = G(+\infty) = G_0 - \Delta G \tag{3.4}$$

[2] 8 keV X-rays produce ~222 or ~300 primary electrons on average in Ne-based or Ar-based gas mixtures [23], respectively, per interaction.



2018 JINST 13 P01015

The quality of the fit of eq. (3.3) indicates upon a good agreement ($\chi^2$/n.d.f. = 0.71) to the simulation (n.d.f., number of degrees of freedom, being the number of iterations). The exponential model is driven by the assumption that the amount of the accumulated charges is proportionally decreasing with the amount of charges attached to the insulating surfaces. In figure 5, after about ~100 min, the gain reaches a plateau, indicating that the ongoing charge accumulation is no longer capable of modifying the electric field in a way that could affect the gain because the electric fields due to new incoming electrons and ions cancel each other.

Using the formalism above, one can define a *characteristic charge*, $Q_{\text{tot}}$ — the total charge, which pass through the THGEM holes during the relaxation period ($\tau$):

$$Q_{\text{tot}} = q_{\text{e}} \times n_{\text{p}} \times R \times \int_0^{\tau} G(t)dt = q_{\text{e}} \times n_{\text{p}} \times R \times \tau \times \left(G_0 - \frac{\Delta G}{e}\right) \tag{3.5}$$

where $q_{\text{e}}$ is the electron charge.

Replacing the *characteristic time* by *characteristic number of iterations* ($\tau_{\text{iter}}$), using eq. (3.3), one can rewrite eq. (3.5) in terms of the *step-size* and $\tau_{\text{iter}}$:

$$Q_{\text{tot}} = q_{\text{e}} \times s \times \tau_{\text{iter}} \times \left(G_0 - \frac{\Delta G}{e}\right) \tag{3.6}$$

The choice of the *step-size* $s$ is an important parameter for simulation convergence. An example of simulation results of THGEM detector, in Ne/$CH_4$(5%) gas mixture with the parameters: $t$=0.4 mm, $a$=1 mm, $d$=0.5 mm, and no-rim, with different *step-size* values (from $0.5 \times 10^6$ to $40 \times 10^6$) is shown in figure 6. The behaviour of the gain $G(t)$ should remain unchanged, regardless the *step-size*. In figure 6a and 6b the fitted $\tau$ is similar, while in figure 6b and 6c clearly show that higher *step-size* lead to different trends.

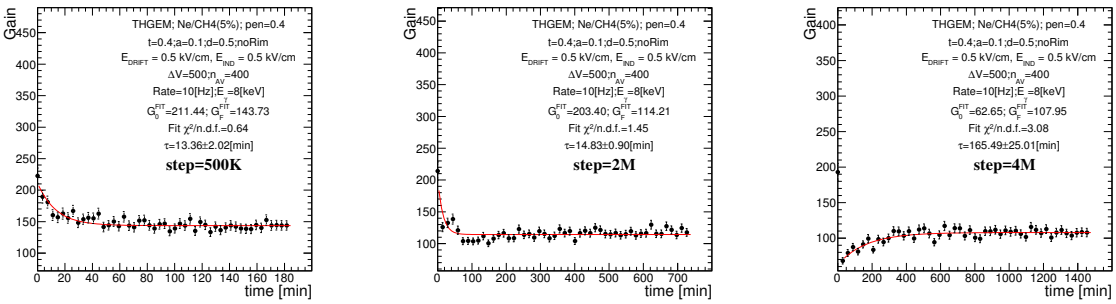


(a) (b) (c)

**Figure 6.** Simulation results of gain stabilization for different step-size values. (a) Gradual decrease of gain due to moderate step-size, (b) the electrode fully charges up after the first iteration, (c) too large step-size.

### 3.3 Convergence rules

Since the *step-size* should not affect the gain over time, a plot of the gain stabilization over time, simulated for different *step-size* values from $0.1 \times 10^6$ to $0.5 \times 10^6$, for the same detector geometry, is shown in the figure 7a, only for those *step-size* values that do not vary the gain trend. According



2018 JINST 13 P01015

to the results obtained in figure 6a, for a step size of $0.5 \times 10^6$ the gain stabilizes after about 3-4 iterations, therefore the step-size was reduced by a factor of 5 to inspect the gain stabilization over 50 simulated iterations. From these curves, the average fitted $\tau$ is $(13 \pm 2)$ min. The plot of $1/\tau_{\text{iter}}$ as a function of $q_e \times s \times (G_0 - \frac{\Delta G}{e})$, depicted in the figure 7b, allows to calculate the value of $Q_{\text{tot}} \approx 58$ pC.

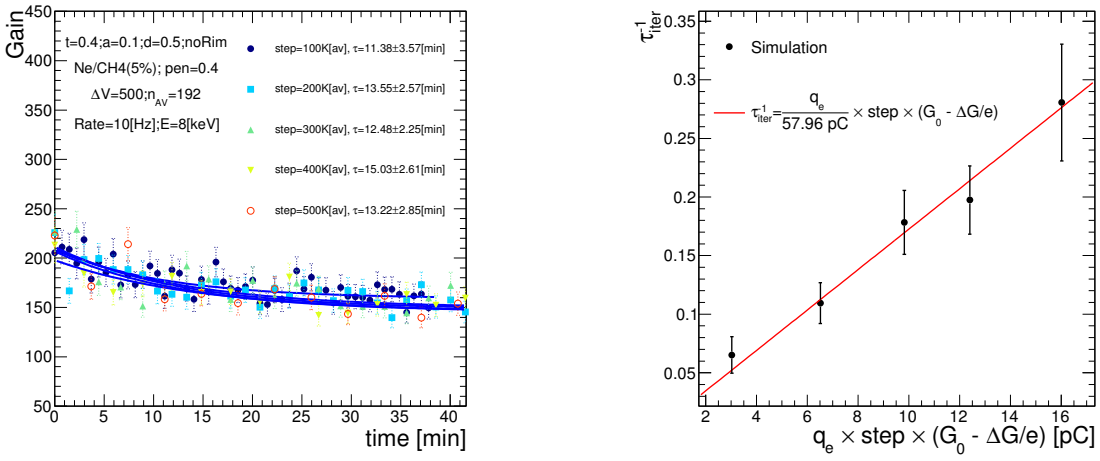


(a) (b)

**Figure 7.** (a) Simulated gain stabilization in the THGEM detector, calculated in the time domain, the solid blue lines are the fitted exponential curves (from eq. (3.3)). (b) The linear relation between the characteristic times in iteration domain vs the *step-size*.

## 4 Results

### 4.1 Voltage effect on gain stabilization

Simulations were performed at different THGEM operation voltages, in the range $\Delta V_{\text{THGEM}} = 500$–$1100$ V, aiming at investigating their influence on gain evolution. To compare the gain evolution for a broader range of $\Delta V_{\text{THGEM}}$ values, the simulation was performed for different gas mixtures (with the highest operation voltages in Ar mixtures).

In figure 8, the calculated $Q_{\text{tot}}$ value (obtained from eq. (3.6)) increases with voltage, indicating that the higher the voltage, the higher the irradiation rate (or time) is needed to reach gain stabilization.

### 4.2 Electrode-thickness effect on the gain stabilization

Gain stabilization was simulated for THGEM electrodes of different thickness, in Ne/$CH_4$(5%) and Ar/$CO_2$(5%) (Ar-based mixtures have about two-fold higher operational voltages, and lower transverse electron diffusion for electric fields below 10 kV cm$^{-1}$ [17]). The $Q_{\text{tot}}$ value calculated from the charging-up of THGEM hole walls and the fraction of the avalanche charges attached to the THGEM walls for an uncharged electrode are shown in table 1.

An increase of the $Q_{\text{tot}}$ is observed with the decrease of the electrode thickness; it is found to be more pronounced than the dependence on the THGEM voltages or electron transport parameters,



2018 JINST 13 P01015

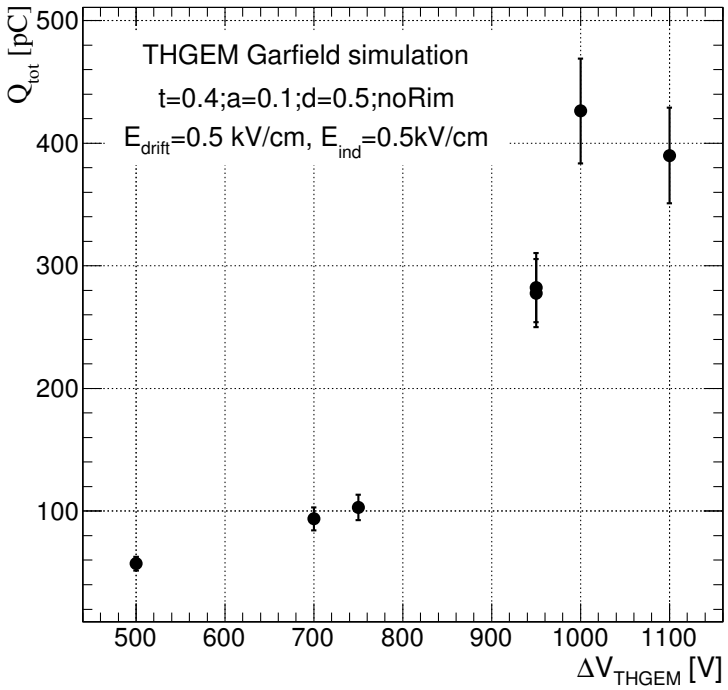


**Figure 8.** Simulated $Q_{\text{tot}}$ for different applied voltages across the THGEM. The $Q_{\text{tot}}$ is calculated according to eq. (3.6). The error bars indicate the spread of calculated $Q_{\text{tot}}$ values among few tens of simulations with varying *step-size*.

**Table 1.** The simulated $Q_{\text{tot}}$ for different electrode thickness and operation voltages and the fraction (in %) of the avalanche charge for uncharged THGEM electrode that accumulates on the THGEM-hole walls.

| Gas | Thickness | $\Delta V_{\text{THGEM}}$ | $G_0$ | $Q_{\text{tot}}$ [pC] | Fraction [%] |
|---|---|---|---|---|---|
| Ne/$CH_4$(5%) | 0.4 | 450 | 80 | 48.11 | 23.4±1.8 |
| Ne/$CH_4$(5%) | 0.4 | 500 | 220 | 57.14 | 23.1±1.8 |
| Ne/$CH_4$(5%) | 0.8 | 600 | 110 | 34.25 | 31.9±0.8 |
| Ne/$CH_4$(5%) | 1.2 | 750 | 130 | 30.43 | 38.0±0.7 |
| Ar/$CO_2$(5%) | 0.4 | 950 | 120 | 277.75 | 18.3±0.3 |
| Ar/$CO_2$(5%) | 0.8 | 1300 | 130 | 130.61 | 22.9±1.4 |

e.g. for thicker structures, and higher applied voltages, a lower total charge value would be needed for modifying the gain. For thicker electrodes, the fraction of accumulated charges on the THGEM holes is larger, due to a broader transverse expansion of the avalanche.



2018 JINST 13 P01015

## 5 Conclusions

The present study introduced a new toolkit for charging-up calculations in MPGDs that can be included in a future version of Garfield++; it is expected to ease simulations of phenomena occurring in gas-avalanche detectors. A case-study is shown, where the new toolkit was used to model the gain stabilization due to charging-up effects in THGEM detectors; a quantitative study was conducted to characterize various aspects of these effects. The gain stabilization typically occurs in a few minutes to a few tens of minutes, depending on several parameters of the THGEM-electrodes. Higher voltages applied across the THGEM-electrode require a larger amount of charge to modify the electric field within the detector holes, resulting in longer gain-stabilization characteristic times. On the other hand, in thicker electrodes, the avalanche is broader due to the expansion of the avalanche-electrons within the holes, and the charging-up of the electrode's insulating surface occurs faster. Most of the simulation studies were carried at relatively low operation voltages (low gains). Differently to GEM detectors with single-conical or double-conical geometry, where the gain stabilization exhibits an increase over time, in THGEM electrodes with cylindrical holes, the effect is a decrease of the detector gain due to a different charge distribution along the hole's surface. A typical characteristic charging-up time in THGEM electrodes is found to be equivalent to a total irradiated charge of hundreds of pC similarly to the values reported for the GEM electrodes with double-conical geometry. The simulation results of the initial decrease of the gain are found to be in a good agreement with previously reported experimental data [5, 6]. Further experimental studies are in course to validate our charging-up model.


## Acknowledgments

This research was supported in part by the I-CORE Program of the Israel Planning and Budgeting Committee, the Nella and Leon Benoziyo Center for High Energy Physics at the Weizmann Institute of Science and by projects PTDC/FIS-NUC/2525/2014 and CERN/FIS-INS/0025/2017 through COMPETE, FEDER and FCT (Lisbon) programs. C.D.R. Azevedo and P.M.M. Correia were supported by FCT (Lisbon) grants SFRH/BPD/79163/2011 and PD/BD/52330/2013 and by I3N laboratory, funded by UID/CTM/50025/2013.


## References


[1] B. Azmoun et al., *A study of gain stability and charging effects in GEM foils*, *IEEE Nucl. Sci. Symp. Conf. Rec.* (2006) 3847.

[2] F. Simon et al., *Development of tracking detectors with industrially produced GEM foils*, *IEEE Trans. Nucl. Sci.* **54** (2007) 2646.

[3] F. Sauli, *The Gas Electron Multiplier (GEM): operating principles and applications*, *Nucl. Instrum. Meth.* **A 805** (2016) 2.

[4] M. Cortesi et al., *THGEM operation in Ne and Ne/$CH_4$*, 2009 *JINST* **4** P08001 [arXiv:0905.2916].

[5] M. Cortesi, J. Yurkon and A. Stolz, *Operation of a THGEM-based detector in low-pressure helium*, 2015 *JINST* **10** P02012 [arXiv:1501.03462].




2018 JINST 13 P01015

[6] M. Cortesi, J. Yurkon, W. Mittig, D. Bazin, S. Beceiro-Novo and A. Stolz, *Studies of THGEM-based detector at low-pressure hydrogen/deuterium, for AT-TPC applications*, 2015 *JINST* **10** P09020 [arXiv:1511.05816].

[7] M. Alexeev et al., *Development of THGEM-based photon detectors for Cherenkov imaging counters*, 2010 *JINST* **5** P03009.

[8] R. Chechik, M. Cortesi, A. Breskin, D. Vartsky, D. Bar and V. Dangendorf, *Thick GEM-like (THGEM) detectors and their possible applications*, *eConf* **C 0604032** (2006) 0025 [physics/0606162].

[9] D. Shaked Renous, A. Roy, A. Breskin and S. Bressler, *Gain stabilization in micro pattern gaseous detectors: methodology and results*, 2017 *JINST* **12** P09036 [arXiv:1707.04356].

[10] M. Alexeev et al., *The gain in thick GEM multipliers and its time-evolution*, 2015 *JINST* **10** P03026.

[11] M. Alfonsi et al., *Simulation of the dielectric charging-up effect in a GEM detector*, *Nucl. Instrum. Meth.* **A 671** (2012) 6.

[12] CERN RD-51 collaboration, P.M.M. Correia et al., *A dynamic method for charging-up calculations: the case of GEM*, 2014 *JINST* **9** P07025 [arXiv:1401.4009].

[13] LUX collaboration, D.S. Akerib et al., *3D modeling of electric fields in the LUX detector*, 2017 *JINST* **12** P11022 [arXiv:1709.00095].

[14] *Garfield++ webpage*, http://cern.ch/garfieldpp/.

[15] P.M.M. Correia and M. Pitt, *Charging-up algorithm for Garfield++ webpage*, https://github.com/pmcorreia/Garfpp-chargingup.git, (2017).

[16] C.A.B. Oliveira et al., *Simulation of VUV electroluminescence in micropattern gaseous detectors: the case of GEM and MHSP*, 2012 *JINST* **7** P09006 [arXiv:1206.1646].

[17] *Magboltz webpage*, http://cern.ch/magboltz.

[18] S.F. Biagi, *Monte Carlo simulation of electron drift and diffusion in counting gases under the influence of electric and magnetic fields*, *Nucl. Instrum. Meth.* **A 421** (1999) 234.

[19] W.P. Jesse and J. Sadauskis, *Alpha-particle ionization in mixtures of the noble gases*, *Phys. Rev.* **88** (1952) 417.

[20] C.D.R. Azevedo, P.M.M. Correia, L.F.N.D. Carramate, A.L.M. Silva and J.F.C.A. Veloso, *THGEM gain calculations using Garfield++: solving discrepancies between simulation and experimental data*, 2016 *JINST* **11** P08018 [arXiv:1606.04852].

[21] Ö. Şahin, I. Tapan, E.N. Özmutlu and R. Veenhof, *Penning transfer in argon-based gas mixtures*, 2010 *JINST* **5** P05002.

[22] Ö. Şahin, T.Z. Kowalski and R. Veenhof, *High-precision gas gain and energy transfer measurements in Ar-$CO_2$ mixtures*, *Nucl. Instrum. Meth.* **A 768** (2014) 104.

[23] F. Sauli, *Principles of operation of multiwire proportional and drift chambers*, CERN-77-09, CERN, Geneva Switzerland, (1977), pg. 92.

2018 JINST 13 P01015